Life Sciences 224 (2019) 204–211

Contents lists available at ScienceDirect

Life Sciences

journal homepage: www.elsevier.com/locate/lifescie

Znhit1 inhibits breast cancer by up-regulating PTEN to deactivate the PI3K/Akt/mTOR pathway

Chunguo Cui[a], Sijie Li[b], Di Wu[b,*]

[a] Department of Breast Surgery, China-Japan Union Hospital of Jilin University, Changchun 130031, China
[b] Department of Breast Surgery, The First Hospital of Jilin University, Changchun 130021, China

ARTICLE INFO

Keywords:
Breast cancer
Znhit1
PTEN
PI3K/Akt/mTOR
Prognosis

ABSTRACT

Aims: Breast cancer (BC) is the most frequently diagnosed cancer, ranking sixth as the cause of death among females in China. Zinc finger HIT-type containing 1 (Znhit1) is a pivotal factor for inhibition of gene mutation and cell proliferation. Due to the unknown function of Znhit1 in cancers, we aimed to explore the role of Znhit1 in BC as well as the underlying mechanisms.

Main methods: Znhit1 expression in clinical specimens and cell lines of BC was measured by quantitative reverse transcription PCR and Western blot analysis. Then, the effects of Znhit1 overexpression on cell proliferation, apoptosis and invasion of BC cells as well as *in vivo* tumor growth were assessed. The interactions among Znhit1, PTEN and the downstream PI3K/Akt/mTOR pathway were evaluated by Western blot analysis. Finally, the role of Znhit1 in prognosis was analyzed in clinical specimens.

Key findings: Znhit1 was down-regulated in BC cell lines and clinical specimens. Znhit1 overexpression induced apoptosis and repressed proliferation and invasion of BC cells. Moreover, Znhit1 overexpression induced cell cycle arrest at G0/G1 stage. *In vivo* data showed that Znhit1 overexpression inhibited BC tumor growth in mice. Further experiments showed Znhit1 affected BC through up-regulating PTEN, along with inactivation of the PI3K/Akt/mTOR pathway. We finally proved that high expression of Znhit1 indicated improved prognosis.

Significance: Znhit1 overexpression inhibited BC tumorigenesis possibly through PTEN-mediated inactivation of the PI3K/Akt/mTOR pathway. Additionally, high expression of Znhit1 indicated improved prognosis.

1. Introduction

With the aging population and prevalence of risk factors, human cancer becomes a huge burden on society worldwide [1]. Globally, breast cancer (BC) is the second most common cancer, accounting for 12% of all cancer incidences in 2012 [2]. Currently, BC is identified to be the most frequently diagnosed cancer, ranking sixth as the cause of death among females in China [3]. Although the understanding of tumor-intrinsic genomic changes has been improved recently, whether a patient is accompanied by high risk of disease recurrence or metastasis remains difficult to define [4].

DNA double-strand breaks (DSBs) are serious events that lead to mutations and chromosomal instability if unrepaired or repaired incorrectly [5]. In vertebrates, DSBs can be repaired by homologous recombination, in which extensive DNA-end resection is required [5–7]. Zinc finger HIT-type containing 1 (Znhit1), located at breakpoint region of chromosome 7, is a component of SNF-2 related CBP activator protein (SRCAP) complex, which has been reported to promote DNA-end resection [8,9]. To be specific, SRCAP complex is capable of remodeling chromatin by catalyzing the incorporation of H2AZ-H2B dimers into nucleosomes [10,11]. Thus, Znhit1 is a pivotal factor for inhibition of gene mutation. Considering that mutation of genes, such as TP53, BRCA1 and BRCA, has been identified in patients with BC [12,13], we hypothesized that there might be an emerging relationship between Znhit1 and BC progression.

As a malignant tumor, BC is characterized by the imbalanced cell proliferation and apoptosis [14]. Moreover, patients with BC are at high risk of recurrence in metastatic form of cancer [15]. Hence, the roles of Znhit1 in BC cell proliferation, apoptosis and invasion are of great importance. The phosphoinositide 3-kinase (PI3K)/Akt/mammalian target of rapamycin (mTOR) pathway is a complex intracellular pathway which is involved in BC and its activation promotes cell growth and tumor progression [16]. Phosphatase and tensin homolog on chromosome ten (PTEN) is a tumor suppressor that is inactivated in human BC [17]. Numerous literatures focused on this protein to explore potential therapeutic strategies for BC [18,19]. The interactions

* Corresponding author at: Department of Breast Surgery, The First Hospital of Jilin University, No.71 Xinmin Street, Changchun 130021, China.
E-mail address: wudi0028lby@sina.com (D. Wu).

https://doi.org/10.1016/j.lfs.2019.03.067
Received 26 December 2018; Received in revised form 26 March 2019; Accepted 26 March 2019
Available online 27 March 2019
0024-3205/

between Znhit1 and PTEN as well as the PI3K/Akt/mTOR pathway are still not fully understood.

In our study, the expression of Znhit1 in BC clinical specimens and BC cell lines was measured. Then, we assessed the effects of abnormally expressed Znhit1 on BC cell proliferation, apoptosis and invasion as well as *in vivo* BC tumor growth. Afterwards, the interactions between Znhit1 and PTEN as well as the PI3K/Akt/mTOR pathway were explored both *in vitro* and *in vivo*. The effects of Znhit1 on survival of patients with BC were also studied.

2. Materials and methods

2.1. Cell culture

Normal breast epithelial cell line MCF-10A and six BC cell lines including MCF7, ZR-75-30, T47D, BT474, SKBR3 and ZR751 were obtained from the American Type Culture Collection (ATCC, Manassas, VA, USA). MCF-10A cells were maintained in DMEM/F-12 medium (GIBCO, Grand Island, NY, USA) with several additives including horse serum (5%; GIBCO), epidermal growth factor (20 ng/mL; Peprotech, Rocky Hill, NJ, USA), hydrocortisone (0.5 μg/mL; Sigma-Aldrich, St. Louis, MO, USA), insulin (10 μg/mL; Sigma-Aldrich), cholera toxin (0.1 μg/mL; Sigma-Aldrich). Base medium for SKBR3 cells was DMEM/F-12 medium, however, for other BC cells was RPMI-1640 medium (GIBCO). Culture medium for all the BC cells was supplemented with 10% fetal bovine serum (FBS; GIBCO). In addition, for T47D cells, 0.2 U/mL of bovine insulin (Sigma-Aldrich) was also added. All cells were grown in a humidified incubator with 5% CO_2 at 37 °C.

2.2. Clinical specimen collection

Human BC tissues and corresponding non-tumor tissues (n = 60) were collected from patients who underwent surgical resection in China-Japan Union Hospital of Jilin University and The First Hospital of Jilin University between February 2008 to January 2010. Patients did not receive any therapy before surgery. Postoperative follow-up information was obtained from the clinical records and patients were followed up for 78 months. Written informed consents were signed prior to sample collection. Surgical tissues were partially transferred to the laboratory in cold temperature for preparation of single cell suspension, and the rest of tissues were snap-frozen in liquid nitrogen immediately, followed by store at −80 °C for subsequent experiments. The procedure was approved by the ethics committee of the China-Japan Union Hospital of Jilin University and The First Hospital of Jilin University. Recurrence-free survival (RFS) was defined as time from the date of surgery to the date of local recurrence or newly diagnosed metastasis.

2.3. Plasmids construction and small interfering RNA (siRNA) synthesis

Full-length Znhit1 sequence was inserted into pcDNA3.1 plasmid (Invitrogen, Carlsbad, CA, USA) and the recombined plasmid was referred to as pc-Znhit1. siRNA targeting PTEN (si-PTEN) was synthesized by GenePharma Co. (Shanghai, China). Plasmids or siRNAs were transfected into MCF7 and T47D cells using the Lipofectamine reagent (Invitrogen) following the protocol of the manufacturer. Cells transfected with siRNAs were harvested at 72 h post-transfection. Stable cell clones were generated after three weeks of selection in culture medium containing 0.5 mg/mL G418 (Sigma-Aldrich).

2.4. Apoptosis assay

Cell apoptosis of transfected cells was measured using double-staining with fluorescein isothiocyanate (FITC)-conjugated Annexin V and propidium iodide (PI). In brief, stably transfected cells (1×10^5) were collected, washed and resuspended in binding buffer. Cells were stained by Annexin V-FITC and PI by using a FITC Annexin V apoptosis detection kit (BD Biosciences, Franklin Lakes, NJ, USA). Cells were detected by a FACS can (Beckman Coulter, Fullerton, CA, USA) and the percentage of apoptotic cells was analyzed by using FlowJo software (Tree Star, San Carlos, CA, USA).

2.5. Cell viability assay

Cell viability of transfected cells was assessed by 3-(4,5-dimethylthiazol-2-yl)-2,5-diphenyltetrazolium bromide (MTT) colorimetric assay. In brief, stably transfected cells were seeded into 96-well plates with a density of 5×10^3 cells/well and maintained at 37 °C. Then, 20 μL of MTT (5 mg/mL; Sigma-Aldrich) was added into each well. After that, the cells were incubated at 37 °C for 4 h, followed by addition of dimethyl sulfoxide (DMSO; 200 μL). After being shaken vigorously for 10 min, the plates were sent to a plate reader (Bio-Rad, Hercules, CA, USA) for measurement at a wavelength of 570 nm.

2.6. Colony formation assay

Cell proliferation was assessed according to the colony formation assay. In brief, 1×10^3 stably transfected cells were seeded into 6-well plates. After 14 days' incubation at 37 °C, cells were fixed with 2% formalin and stained by 0.5% crystal violet (Sigma-Aldrich). Then, colonies containing > 50 cells were counted under a light microscopy (Olympus, Tokyo, Japan).

2.7. Assessment of cell cycle progression

The distribution of cells in three phases (G2/M, G and G0/G1) of cell-cycle progression was tested by PI staining and flow cytometric analysis. Briefly, 1×10^5 cells following transfection were collected and suspended in chilled 70% ethanol at 4 °C overnight. The cells were stained by 50 μg/mL PI (Sigma-Aldrich) for 30 min at room temperature in the presence of 0.1% Triton X-100 (Sigma-Aldrich) and 20 μg/mL RNase A (Beyotime, Shanghai, China). FlowJo software (Tree Star) was utilized to analyze the sample.

2.8. Transwell invasion assay

Z-VAD-FMK, a pan-caspase inhibitor which can block all features of apoptosis, was purchased from Selleck Chemicals (Houston, TX, USA). 100 μM Z-VAD-FMK was used to treat cell for 2 h prior to transfection. Cell invasion of transfected cells was determined by invasion Transwell assay. The Transwell inserts were pre-coated with 50 μg Matrigel (BD Biosciences). In brief, 200 μL serum-free medium containing 1×10^5 cells were seeded into the upper chambers, whereas the lower chamber was filled with 600 μL complete medium. After incubation at 37 °C for 24 h, cells that did not invade were removed carefully, and the invading cells were fixed and stained with crystal violet, followed by counting under a microscope.

2.9. Mouse xenograft models

Five-week-old nude female mice weighing 17–19 g were purchased from Charles River Laboratories International, Inc. (Beijing, China). Mice were maintained with rodent chow and water *ad libitum* on a standard 12 h light/dark cycle. Mice were randomly assigned into two groups (n = 6), and then 5×10^6 MCF7 cells in PBS, stably transfected with pcDNA3.1 or pc-Znhit1, were injected subcutaneously into the right flank of mice. By using external calipers, length (l) and width (w) of tumors were measured every week and tumor volume was calculated on the basis of the formula (tumor volume = $l \times w^2 \times 0.52$). Four weeks later, tumors were dissected and weighed. All the procedure was approved by the ethics committee of China-Japan Union Hospital of Jilin University.

2.10. Ki67$^+$ staining of cells from clinical specimens

Fresh isolated surgical tissues were cut into small pieces, washed in PBS and digested in collagenase IV (Sigma-Aldrich). After incubation at 37 °C for 2 h, single cell suspensions were obtained after careful filtration through Nylon meshes (sterile, 7.4-μm aperture). Then, cells were fixed in formaldehyde and stained according to the recommendation of the Ki67 staining kit (558616, BD Pharmingen, San Jose, CA, USA). Stained cells were analyzed using a FACS can (Beckman Coulter) and data were analyzed using FlowJo Software (Tree Star).

2.11. Quantitative reverse transcription PCR (qRT-PCR)

Total RNA of cells and tissues was extracted using RNeasy (QIAGEN Inc., Valencia, CA, USA) following the manufacturer's suggestion. The RNA yield was determined by the ratio of A260/A280. By using a Multiscribe RT kit (Applied Biosystems, Foster City, CA, USA) according to the manufacturer's protocol, 500 ng RNA was reversely transcribed to cDNA. Then, cDNA (50 ng) was acted as template for quantitative PCR with a Taqman Universal Master Mix II (Applied Biosystems) following the manufacturer's protocol. The thermal cycling parameters were 10 min at 95 °C, followed by 40 cycles of 15 s at 95 °C and 1 min at 60 °C. Relative expression of Znhit1 mRNA was calculated using the $2^{-\Delta\Delta Ct}$ method [20]. GAPDH acted as the housekeeping gene.

2.12. Western blot analysis

Whole cell lysates from tissues and cells were prepared by using RIPA lysis buffer (Beyotime). After quantification using BCA™ Protein Assay Kit (Pierce, Rockford, IL, USA), supernatants of cell lysates were separated by 10% SDS-PAGE and transferred onto polyvinylidene difluoride (PVDF) membranes. These membranes were blocked by 5% skimmed milk, followed by incubation at 4 °C overnight with the presence of primary antibody against Znhit1 (A12010, Boster Biological Technology, Wuhan, China), c-Myc (ab122907), cyclinD1 (ab134175), p21 (ab109520), cleaved caspase-3 (ab49822), E-cadherin (ab15148), PTEN (ab32199), eukaryotic initiation factor 4E-binding protein 1 (4E-BP1; ab131453), phospho (p)-4E-BP1 (ab75767), PI3K (ab109006), p-PI3K (ab182651), matrix metalloproteinase (MMP)-2 (ab97779), MMP-9 (ab137867), GAPDH (ab181603, all Abcam), Akt (9272) or p-Akt (9271, both Cell Signaling Technology, Beverly, MA, USA). After rinsing, membranes were incubated with horseradish peroxidase-conjugated secondary antibody (goat anti-rabbit, ab6721, Abcam) at room temperature for 1 h. After rinsing again, the bound antibody was visualized by a SuperSignal West Pico chemiluminescence ECL kit (Pierce).

2.13. Statistical analysis

All experiments were repeated three times. The results were presented as the means ± standard deviation (SD). Statistical analysis was performed using statistical software SPSS 19.0 (SPSS Inc., Chicago, IL, USA). The *P*-values were calculated using the one-way analysis of variance (ANOVA) or unpaired two-tailed *t*-test. Recurrence-free survival curve was calculated using the Kaplan-Meier method, a non-parametric statistic used to estimate the survival function from lifetime data. The difference between low and high Znhit1 expression groups was assessed by log-rank test, a hypothesis test to compare the survival distributions of two samples. A $P < 0.05$ was considered as a significant difference.

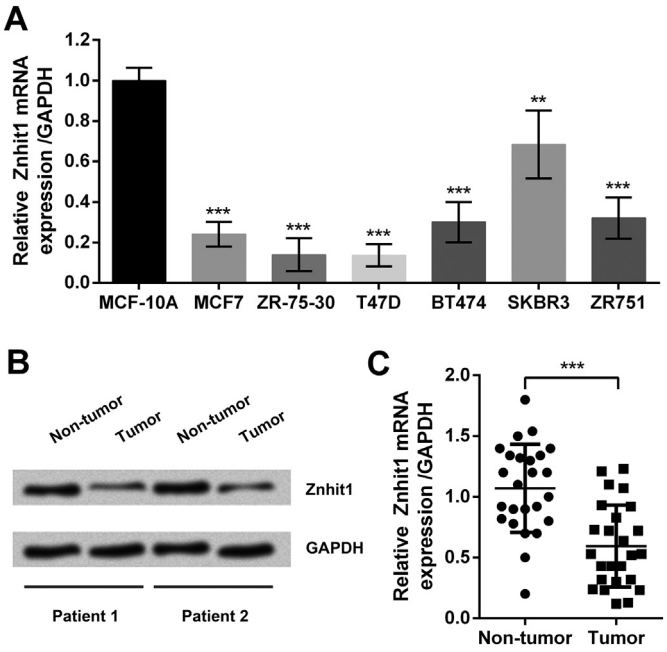

Fig. 1. Znhit1 is down-regulated in breast cancer (BC) cell lines and clinical specimens of BC. mRNA and protein expression of Znhit1 was measured by quantitative reverse transcription PCR and Western blot analysis, respectively. A. Relative mRNA expression of Znhit1 in normal MCF-10A cells and six BC cell lines. B. Representatives of Znhit1 protein expression in tumor tissues and paired non-tumorous tissues (n = 2). C. Relative mRNA expression of Znhit1 in tumor tissues and paired non-tumorous tissues (n = 25). Data are presented as the mean ± SD. $^{**}P < 0.01$; $^{***}P < 0.001$. Znhit1, Zinc finger HIT-type containing 1.

3. Results

3.1. Znhit1 expression was down-regulated in BC cell lines and clinical tissues

The mRNA expression of Znhit1 in normal MCF-10A cells and six BC cell lines was measured by qRT-PCR. In Fig. 1A, mRNA expression of Znhit1 in BC cells was significantly lower than that in normal MCF-10A cells ($P < 0.01$ or $P < 0.001$). Meanwhile, mRNA and protein expression of Znhit1 in clinical tissues was also assessed. Results showed protein (Fig. 1B) and mRNA (Fig. 1C) expression of Znhit1 was significantly lower in tumor tissues compared with that in non-tumorous tissues ($P < 0.001$). All the results illustrated that Znhit1 expression was down-regulated in BC.

3.2. Overexpression of Znhit1 induced apoptosis and repressed proliferation and invasion in BC cells

Recombined plasmids were stably transfected into MCF7 and T47D cells to overexpress Znhit1. Fig. 2A showed protein expression of Znhit1 in the MCF7 and T47D cells was markedly up-regulated by transfection with pc-Znhit1, suggesting that Znhit1 was overexpressed after stable transfection. The expression of proteins associated with cell proliferation, apoptosis and invasion were measured. In Fig. 2B, Znhit1 overexpression down-regulated expression of c-Myc and cyclinD1 while up-regulated expression of p21, cleaved caspase-3 and E-cadherin. Then, flow cytometry results showed percentage of apoptotic cells was dramatically increased by Znhit1 overexpression as compared to the pcDNA3.1 group in both MCF7 and T47D cells ($P < 0.01$ or $P < 0.001$, Fig. 2C). In MCF7 cells, cell viability was significantly reduced by Znhit1 overexpression as compared to the pcDNA3.1 group at 2 d ($P < 0.05$), 3 d and 4 d (both $P < 0.01$) after cell culture (Fig. 2D).

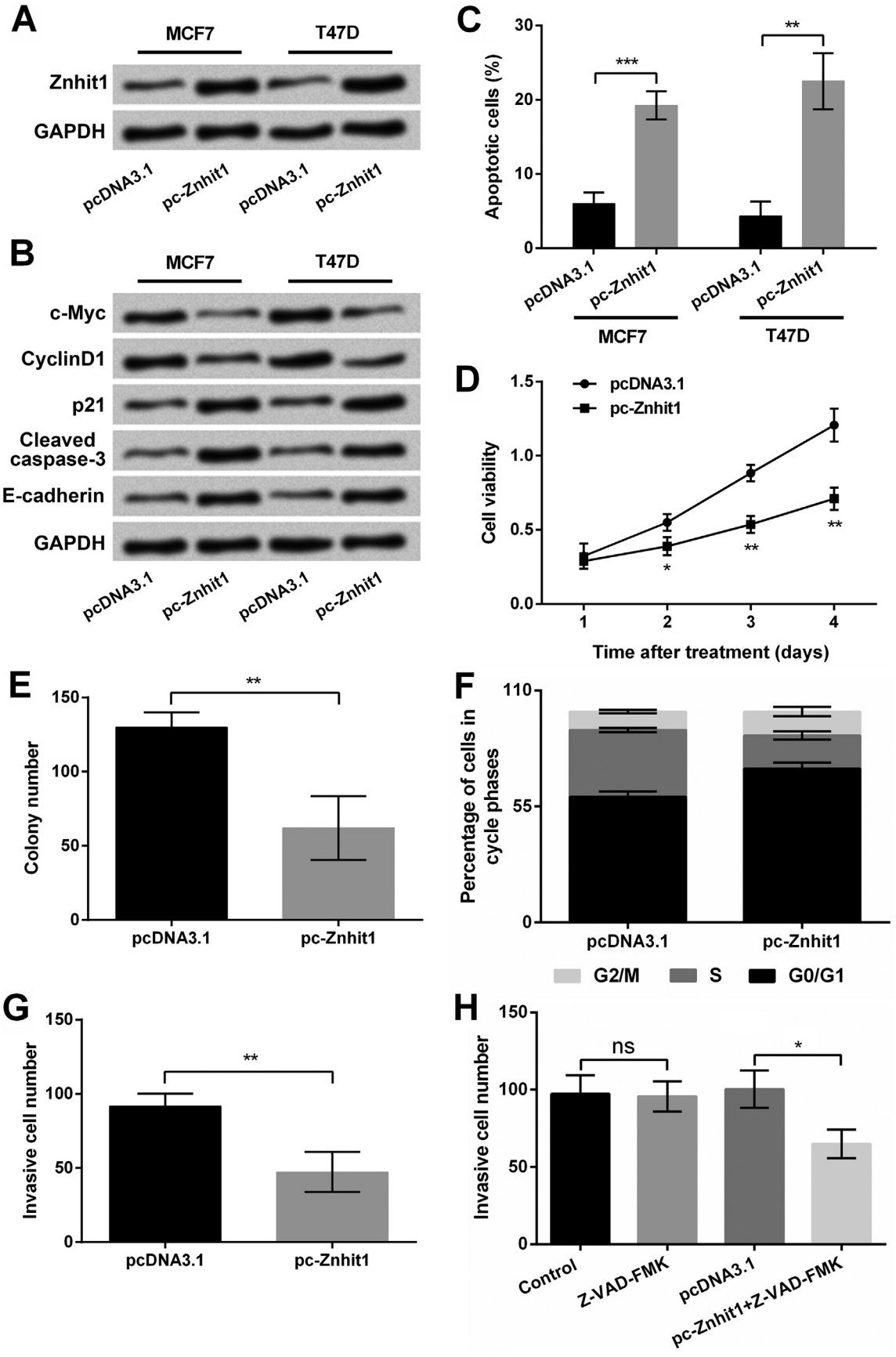

(caption on next page)

Fig. 2. Znhit1 overexpression induces apoptosis and represses proliferation and invasion of breast cancer cells. A. Protein expression of Znhit1 in stably transfected MCF7 and T47D cells by Western blot analysis. B. Expression of proteins associated with cell proliferation, apoptosis and invasion in stably transfected MCF7 and T47D cells by Western blot analysis. C. Percentage of apoptotic cells in stably transfected MCF7 and T47D cells by flow cytometry. D. Cell viability of stably transfected MCF7 cells by MTT assay. E. Colony number of stably transfected MCF7 cells. F. Cell cycle distribution of stably transfected MCF7 cells. G. Invasive cell number of stably transfected MCF7 cells by Transwell assay. H. Invasive cell number in the presence of an apoptosis inhibitor Z-VAD-FMK. Data are presented as the mean ± SD. ns, no significant. *$P < 0.05$; **$P < 0.01$; ***$P < 0.001$. Znhit1, Zinc finger HIT-type containing 1; MTT, 3-(4,5-dimethylthiazol-2-yl)-2,5-diphenyltetrazolium bromide; pc-Znhit1, pcDNA3.1 plasmid carry full-length Znhit1 sequences.

Likewise, colony number was dramatically decreased by Znhit1 overexpression compared with the pcDNA3.1 group ($P < 0.01$, Fig. 2E). Znhit1 overexpression induced cell cycle arrest at G0/G1 stage as compared to the pcDNA3.1 group (Fig. 2F). Conversely, invasive cell number of cells overexpressing Znhit1 was significantly lower than that of cells transfected with pcDNA3.1 ($P < 0.01$, Fig. 2G). Besides that, apoptosis inhibitor Z-VAD-FMK was used prior to Transwell assay. We found that, cell invasion was also significantly repressed by Znhit1 overexpression in the presence of Z-VAD-FMK ($P < 0.05$, Fig. 2H). The result indicated that cell invasion was indeed inhibited and not because Znhit1 overexpression killed more cells so as to have fewer cells available for Transwell invasion. Taken together, we concluded that Znhit1 overexpression induced apoptosis and inhibited proliferation and invasion of BC cells.

3.3. Overexpression of Znhit1 inhibited in vivo tumor growth

MCF7 cells stably transfected with pcDNA3.1 or pc-Znhit1 were injected into nude mice, followed by assessment of tumor volume and weight. As shown in Fig. 3A, tumor volume of mice was markedly reduced by Znhit1 overexpression at 2 weeks ($P < 0.05$), 3 weeks ($P < 0.01$) and 4 weeks ($P < 0.001$) post-injection. The tumor weight of mice was also dramatically decreased by Znhit1 overexpression at 4 weeks post-injection ($P < 0.01$, Fig. 3B). Western blotting for the Znhit1 expression in dissected tumors proposed that Znhit1 was overexpressed during the tumorigenesis in mice, which were injected with MCF7 cells stably transfected with pc-Znhit1 (Fig. 3C). Results above illustrated that Znhit1 overexpression repressed *in vivo* tumor growth.

3.4. Overexpression of Znhit1 inhibited the PI3K/Akt/mTOR and up-regulated PTEN expression

Expression of PTEN and phosphorylation of key kinases in the PI3K/Akt/mTOR pathways was assessed. In Fig. 4A, PTEN expression was up-regulated while phosphorylated levels of 4E-BP1 (key substrate of mTOR), Akt and PI3K were reduced in both MCF7 and T47D cells. Furthermore, the Znhit1 overexpression induced alterations of these proteins were reversed by PTEN silence (Fig. 4B) in MCF7 cells. Similarly, up-regulation of PTEN and down-regulations of p-4E-BP1, p-Akt and p-PI3K were also observed in tumor tissues of mice injected with Znhit1-overexpressed MCF7 cells (Fig. 4C) and tumor tissues of clinical specimens as well (Fig. 4D). Subsequent experiments showed PTEN expression was positively correlated with Znhit1 expression in tumor tissues of mice (Fig. 4E). Besides, down-regulations of c-Myc and cyclinD1 as well as up-regulations of p21, cleaved caspase-3 and E-cadherin were reversed by PTEN silence (Fig. 4F). Those results suggested that Znhit1 might inhibit neoplasm growth through up-regulating PTEN and inhibiting the PI3K/Akt/mTOR pathway.

3.5. High expression of Znhit1 indicated higher survival

Expression of Znhit1 in clinical specimens was dichotomized into low and high expression groups. Then, prognostic significance of Znhit1 in patients with BC was assessed by Kaplan-Meier analysis and log-rank test. In Fig. 5A, high expression of Znhit1 was identified to be correlated with high recurrence-free survival (n = 20 for each group, $P = 0.042$). Additionally, lower percentage of Ki67 positive cells ($P < 0.05$,

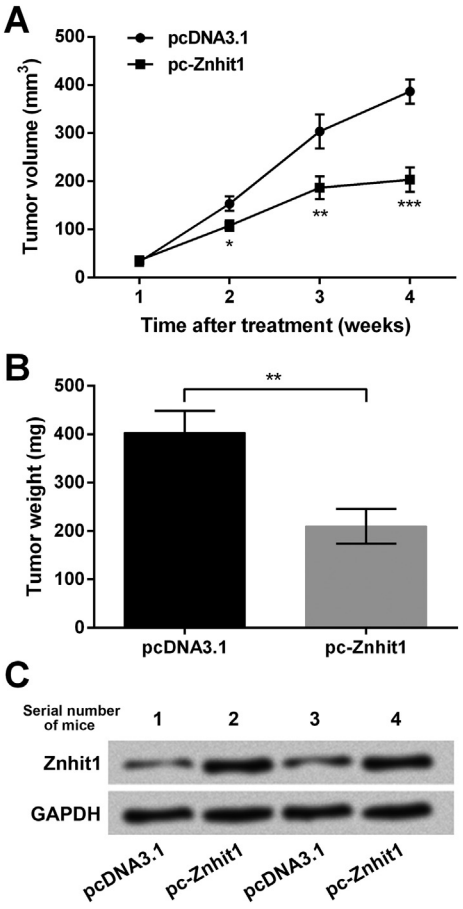

Fig. 3. Znhit1 overexpression represses *in vivo* tumor growth. MCF7 cells stably transfected with pcDNA3.1 or pc-Znhit1 were injected into nude mice, and those mice were fed for 4 weeks. A. Tumor volume of mice at each week post-injection. B. Tumor weight of mice at 4 weeks post-injection. C. Representatives of Znhit1 protein expression by Western blot analysis. Data are presented as the mean ± SD. *$P < 0.05$; **$P < 0.01$; ***$P < 0.001$. Znhit1, Zinc finger HIT-type containing 1; pc-Znhit1, pcDNA3.1 plasmid carry full-length Znhit1 sequences.

Fig. 5B), up-regulated expression of E-cadherin and down-regulated expression of MMP-2 and MMP-9 (Fig. 5C) were observed in patients with high Znhit1 expression compared with the Znhit1-low group (n = 10 for each group). Moreover, Znhit1 expression in patients with stage II cancer was significantly lower than that in patients with stage I cancer while was higher than that in patients with stage III cancer (n = 20 for each group, both $P < 0.05$, Fig. 5D). Those results illustrated that high expression of Znhit1 indicated higher survival.

4. Discussion

Although BC is curable if diagnosed at an early stage, high rate of recurrence (20–30%) makes it become notorious [21]. It is urgently needed to discover novel therapeutic targets for BC. In our study, Znhit1 was found to be down-regulated in BC tissues and cell lines. Overexpression of Znhit1 induced cell apoptosis but repressed cell

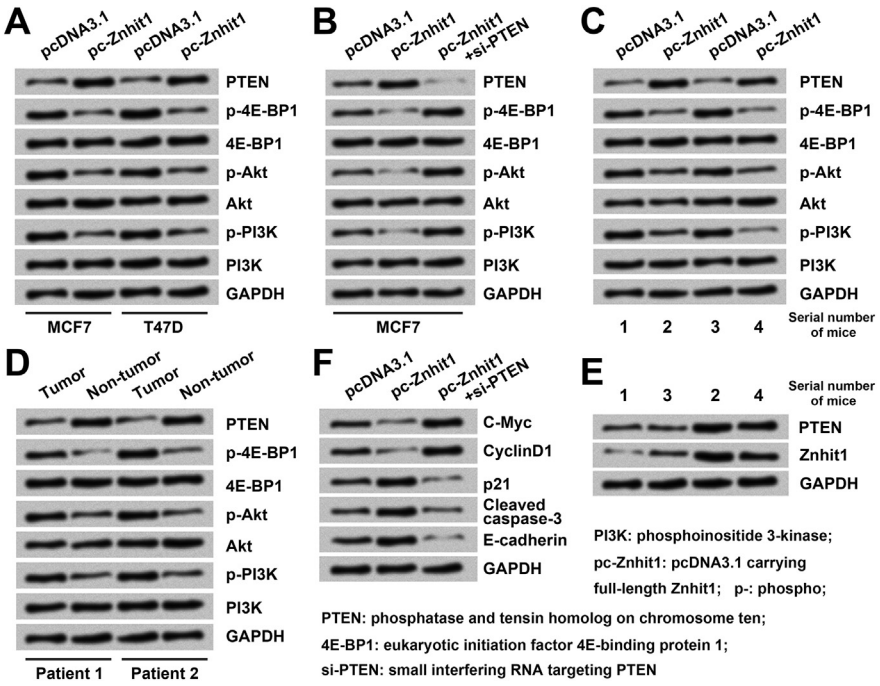

Fig. 4. Znhit1 overexpression up-regulates PTEN and inhibits the PI3K/Akt/mTOR pathway in breast cancer cells. Protein expression was determined by Western blot analysis. A. Znhit1 overexpression up-regulated PTEN and decreased phosphorylation of key kinases in the PI3K/Akt/mTOR pathway in MCF7 and T47D cells. B. Alterations of PTEN expression and phosphorylated levels of key kinases in the PI3K/Akt/mTOR pathway were reversed by PTEN silence in MCF7 cells. C. Up-regulated PTEN expression and decreased phosphorylation of key kinases in the PI3K/Akt/mTOR pathway were observed in tumor tissues of mice. D. PTEN was up-regulated and phosphorylated levels of key kinases in the PI3K/Akt/mTOR pathway were decreased in tumor tissues compared with corresponding non-tumorous tissues of clinical specimens. E. PTEN expression was positively correlated with Znhit1 expression in tumor tissues of mice. F. Alterations of proteins associated with proliferation, apoptosis and invasion were reversed by PTEN silence in MCF-7 cells. Znhit1, Zinc finger HIT-type containing 1.

proliferation and invasion *in vitro*. Mouse xenograft models showed Znhit1 inhibited *in vivo* tumor growth. More experiments proved that Znhit1 affected BC cells through up-regulating PTEN, followed by inactivation of the PI3K/Akt/mTOR pathway. By analyses of the clinical BC tissues, we found high expression of Znhit1 indicated high recurrence-free survival in patients with BC.

The anti-proliferative role of Znhit1 had been reported previously [22]. However, the role of Znhit1 in cancers remains unclear. To explore the possible role of Znhit1 in BC, we measured the expression of Znhit1 in clinical BC tissues and cell lines. Results showed Znhit1 was low expressed in six BC cell lines and clinical BC specimens, suggesting the possible involvements of Znhit1 in BC progression.

To verify whether Znhit1 acted as a tumor suppressor, Znhit1 was overexpressed *via* stable cell transfection. Results in our study showed cell apoptosis was induced while cell proliferation and invasion were both repressed in BC cells. Those results were consistent with the literature by Yang et al., in which, Znhit1 was reported to cause cell cycle arrest and play essential role in cell proliferation [22]. c-Myc is a member of MYC proto-oncogene family that acts as a key regulator in tumor initiation and maintenance [23]. CyclinD1 is a pivotal G1-phase cyclin that binds to CDK4/6, whose activity is required for G1/S transition [24]. Of contrast, p21 is a member of CDK inhibitor family that arrest G1/S transition [25,26]. In our study, the down-regulation of c-Myc and cyclinD1 as well as the up-regulation of p21, induced by

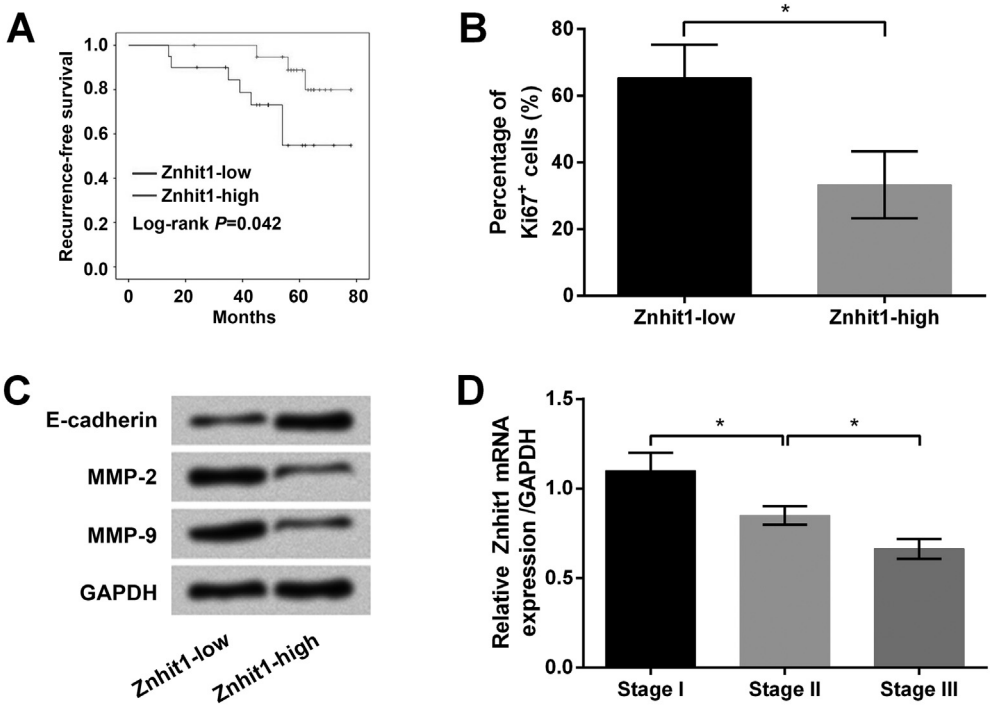

Fig. 5. High expression of Znhit1 indicates improved prognosis. Expression of Znhit1 in clinical specimens was dichotomized into low and high expression groups. A. Kaplan-Meier analysis of recurrence-free survival in patients with breast cancer (n = 20 for each group). B. Percentage of Ki67 positive cells by $Ki67^+$ staining (n = 10 for each group). C. Expression of proteins associated with cell invasion by Western blot analysis (n = 10 for each group). D. Relative mRNA expression of Znhit1 in tumor tissues from patients with stage I–III breast cancer by quantitative reverse transcription PCR (n = 20 for each group). Data are presented as the mean ± SD. $^*P < 0.05$. Znhit1, Zinc finger HIT-type containing 1; MMP, matrix metalloproteinase.

Znhit1 overexpression, partially explained the anti-proliferative role of Znhit1 in BC cells. As a key executor of apoptosis, up-regulated cleaved caspase-3 is the evidence of cell apoptosis [27]. In epithelial cells, E-cadherin is the main cell-to-cell-adhesion molecule and its down-regulation is frequently observed in BC [28]. The up-regulations of cleaved caspase-3 and E-cadherin made by Znhit1 overexpression, provided supports for the elevated apoptosis and reduced invasion in BC cells.

Afterwards, we also explored the *in vivo* role of Znhit1 in BC tumor growth. As a result, volume and weight of tumors synthesized from transfected MCF7 cells were both reduced by Znhit1 overexpression in nude mice. Together, the expression of Znhit1 in tumors was measured, illustrating that the Znhit1 was stably overexpressed during the tumorigenesis in mice. Those *in vivo* results consolidated the tumor suppressive role of Znhit1 in BC.

To further explore the underlying mechanism of Znhit1-associated regulation in BC, expression of PTEN and proteins associated with the PI3K/Akt/mTOR pathway were analyzed. We found that Znhit1 overexpression up-regulated PTEN and inhibited the PI3K/Akt/mTOR pathway in BC cells. Then, the Znhit1-induced alterations were identified to be reversed by PTEN silence, illustrating that Znhit1 inhibited the PI3K/Akt/mTOR cascade possibly through up-regulating PTEN. Subsequently, the effects of Znhit1 overexpression on BC were verified in tumors from mice and clinical specimens. Data from *in vivo* experiments proved the positive correlation between PTEN and Znhit1. Further experiments stated that Znhit1 affected proliferation, apoptosis and invasion of BC cells possibly through up-regulating PTEN.

Utilizing clinical specimens, Znhit1 expression was found to be positive correlated with recurrence-free survival. Ki67 is a nuclear protein which can be observed in all phases of cell cycle except for G0 phase [29]. Ki67 has been reported as a useful biomarker for BC in previous studies and its expression is linked to worse prognosis [30,31]. MMPs are proteases involved in degradation and modulation of extracellular proteins, and their expression lead to tumor initiation and progression [32]. In our study, high expression of Znhit1 was correlated with low expression of Ki67, MMP-2 and MMP-9 as well as high expression of E-cadherin in clinical specimens, suggesting the improved prognosis. Besides, Znhit1 expression was proved to be down-regulated with the increase of stages.

In conclusion, we firstly identified Znhit1 as a tumor suppressor that inhibited tumor growth both *in vitro* and *in vivo*. In addition, Znhit1 was positively correlated with PTEN expression and it could affect BC through PTEN-mediated inhibition of the PI3K/Akt/mTOR pathway. We also proved that high expression of Znhit1 indicated improved prognosis. Our study revealed the possible molecular mechanism for the Znhit1-associated regulation in BC, providing innovate therapeutic strategies for the treatment of BC.

Acknowledgements

None.

Funding

This research received no specific grant from any funding agency in the public, commercial or not-for-profit sectors.

Conflict of interest

The authors declare no conflict of interest.

Authors' contributions

Conceived and designed the experiments: Chunguo Cui and Di Wu; Performed the experiments and analyzed the data: Chunguo Cui; Contributed reagents/materials/analysis tools: Sijie Li; Wrote the manuscript: Chunguo Cui; Revised the manuscript: Di Wu.

References

[1] L.A. Torre, F. Bray, R.L. Siegel, J. Ferlay, J. Lortet-Tieulent, A. Jemal, Global cancer statistics, 2012, CA Cancer J. Clin. 65 (2015) 87–108.
[2] J. Ferlay, I. Soerjomataram, R. Dikshit, S. Eser, C. Mathers, M. Rebelo, D.M. Parkin, D. Forman, F. Bray, Cancer incidence and mortality worldwide: sources, methods and major patterns in GLOBOCAN 2012, Int. J. Cancer 136 (2015) E359–E386.
[3] C. Xia, C. Kahn, J. Wang, Y. Liao, W. Chen, X.Q. Yu, Temporal trends in geographical variation in breast cancer mortality in China, 1973–2005: an analysis of nationwide surveys on cause of death, Int. J. Environ. Res. Public Health 13 (2016) 963.
[4] M. Limoge, A. Safina, A.M. Truskinovsky, I. Aljahdali, J. Zonneville, A. Gruevski, C.L. Arteaga, A.V. Bakin, Tumor p38MAPK signaling enhances breast carcinoma vascularization and growth by promoting expression and deposition of pro-tumorigenic factors, Oncotarget 8 (2017) 61969–61981.
[5] V. Garcia, S.E. Phelps, S. Gray, M.J. Neale, Bidirectional resection of DNA double-strand breaks by Mre11 and Exo1, Nature 479 (2011) 241–244.
[6] P. Huertas, DNA resection in eukaryotes: deciding how to fix the break, Nat. Struct. Mol. Biol. 17 (2010) 11–16.
[7] T. Liu, J. Huang, DNA end resection: facts and mechanisms, Genomics, Proteomics & Bioinformatics 14 (2016) 126–130.
[8] M. McGinity, V. Bartanusz, B. Dengler, L. Birnbaum, J. Henry, Pseudomyogenic hemangioendothelioma (epithelioid sarcoma-like hemangioendothelioma, fibroma-like variant of epithelioid sarcoma) of the thoracic spine, Eur. Spine J. 22 (2013) 506–511.
[9] S. Dong, J. Han, H. Chen, T. Liu, M.S.Y. Huen, Y. Yang, C. Guo, J. Huang, The human SRCAP chromatin remodeling complex promotes DNA-end resection, Curr. Biol. 24 (2014) 2097–2110.
[10] M.M. Wong, L.K. Cox, J.C. Chrivia, The chromatin remodeling protein, SRCAP, is critical for deposition of the histone variant H2A.Z at promoters, J. Biol. Chem. 282 (2007) 26132–26139.
[11] D.D. Ruhl, J. Jin, Y. Cai, S. Swanson, L. Florens, M.P. Washburn, R.C. Conaway, J.W. Conaway, J.C. Chrivia, Purification of a human SRCAP complex that remodels chromatin by incorporating the histone variant H2A.Z into nucleosomes, Biochemistry 45 (2006) 5671–5677.
[12] L. Silwal-Pandit, H.K. Vollan, S.F. Chin, O.M. Rueda, S. McKinney, T. Osako, D.A. Quigley, V.N. Kristensen, S. Aparicio, A.L. Borresen-Dale, C. Caldas, A. Langerod, TP53 mutation spectrum in breast cancer is subtype specific and has distinct prognostic relevance, Clin. Cancer Res. 20 (2014) 3569–3580.
[13] F.J. Couch, S.N. Hart, P. Sharma, A.E. Toland, X. Wang, P. Miron, J.E. Olson, A.K. Godwin, V.S. Pankratz, C. Olswold, S. Slettedahl, E. Hallberg, L. Guidugli, J.I. Davila, M.W. Beckmann, W. Janni, B. Rack, A.B. Ekici, D.J. Slamon, I. Konstantopoulou, F. Fostira, A. Vratimos, G. Fountzilas, L.M. Pelttari, W.J. Tapper, L. Durcan, S.S. Cross, R. Pilarski, C.L. Shapiro, J. Klemp, S. Yao, J. Garber, A. Cox, H. Brauch, C. Ambrosone, H. Nevanlinna, D. Yannoukakos, S.L. Slager, C.M. Vachon, D.M. Eccles, P.A. Fasching, Inherited mutations in 17 breast cancer susceptibility genes among a large triple-negative breast cancer cohort unselected for family history of breast cancer, J. Clin. Oncol. 33 (2015) 304–311.
[14] X. Zhou, G.G. Yue, S.K. Tsui, J. Pu, K.P. Fung, C.B. Lau, Elaborating the role of natural products on the regulation of autophagy and their potentials in breast cancer therapy, Curr. Cancer Drug Targets 18 (2018) 239–255.
[15] E. Al Kubaisy, K. Arafat, O. De Wever, A.H. Hassan, S. Attoub, SMARCAD1 knockdown uncovers its role in breast cancer cell migration, invasion, and metastasis, Expert Opin. Ther. Targets 20 (2016) 1035–1043.
[16] E. Paplomata, R. O'Regan, The PI3K/AKT/mTOR pathway in breast cancer: targets, trials and biomarkers, Ther. Adv. Med. Oncol. 6 (2014) 154–166.
[17] G. Kim, M. Ouzounova, A.A. Quraishi, A. Davis, N. Tawakkol, S.G. Clouthier, F. Malik, A.K. Paulson, R.C. D'Angelo, S. Korkaya, T.L. Baker, E.S. Esen, A. Prat, S. Liu, C.G. Kleer, D.G. Thomas, M.S. Wicha, H. Korkaya, SOCS3-mediated regulation of inflammatory cytokines in PTEN and p53 inactivated triple negative breast cancer model, Oncogene 34 (2015) 671–680.
[18] X. Li, W. Xie, C. Xie, C. Huang, J. Zhu, Z. Liang, F. Deng, M. Zhu, W. Zhu, R. Wu, J. Wu, S. Geng, C. Zhong, Curcumin modulates miR-19/PTEN/AKT/p53 axis to suppress bisphenol A-induced MCF-7 breast cancer cell proliferation, Phytother. Res. 28 (2014) 1553–1560.
[19] F. Ma, J. Zhang, L. Zhong, L. Wang, Y. Liu, Y. Wang, L. Peng, B. Guo, Upregulated microRNA-301a in breast cancer promotes tumor metastasis by targeting PTEN and activating Wnt/β-catenin signaling, Gene 535 (2014) 191–197.
[20] K.J. Livak, T.D. Schmittgen, Analysis of relative gene expression data using real-time quantitative PCR and the 2(−delta delta C(T)) method, Methods 25 (2001) 402–408.
[21] W. Kim, K.S. Kim, R.W. Park, Nomogram of naive Bayesian model for recurrence prediction of breast cancer, Healthc. Inform. Res. 22 (2016) 89–94.
[22] Z. Yang, Y. Cao, X. Zhu, Y. Huang, Y. Ding, X. Liu, Znhit1 causes cell cycle arrest and down-regulates CDK6 expression, Biochem. Biophys. Res. Commun. 386 (2009) 146–152.
[23] M. Vita, M. Henriksson, The Myc oncoprotein as a therapeutic target for human cancer, Semin. Cancer Biol. 16 (2006) 318–330.
[24] Z. Lin, L. Xiong, J. Zhou, J. Wang, Z. Li, H. Hu, Q. Lin, Gamma-glutamylcyclotransferase knockdown inhibits growth of lung cancer cells through G0/G1 phase arrest, Cancer Biother. Radiopharm. 30 (2015) 211–216.
[25] J. Zhang, Y. Yang, L. Lei, M. Tian, Rhizoma Paridis saponins induces cell cycle arrest and apoptosis in non-small cell lung carcinoma A549 cells, Med. Sci. Monit. 21 (2015) 2535–2541.

[26] W.L. Qiao, H.Y. Hu, B.W. Shi, L.J. Zang, W. Jin, Q. Lin, Lentivirus-mediated knockdown of TSP50 suppresses the growth of non-small cell lung cancer cells via G0/G1 phase arrest, Oncol. Rep. 35 (2016) 3409–3418.
[27] L. Yang, Z. Wen, Y. Long, N. Huang, Y. Cheng, L. Zhao, H. Zheng, A H(+)-triggered bubble-generating nanosystem for killing cancer cells, Chem. Commun. (Camb.) 52 (2016) 10838–10841.
[28] M.A. El Sharouni, E.L. Postma, P.J. van Diest, Correlation between E-cadherin and p120 expression in invasive ductal breast cancer with a lobular component and MRI findings, Virchows Arch. 471 (2017) 707–712.
[29] R. Yerushalmi, R. Woods, P.M. Ravdin, M.M. Hayes, K.A. Gelmon, Ki67 in breast cancer: prognostic and predictive potential, Lancet Oncol. 11 (2010) 174–183.
[30] T. Yoshioka, M. Hosoda, M. Yamamoto, K. Taguchi, K.C. Hatanaka, E. Takakuwa, Y. Hatanaka, Y. Matsuno, H. Yamashita, Prognostic significance of pathologic complete response and Ki67 expression after neoadjuvant chemotherapy in breast cancer, Breast Cancer 22 (2015) 185–191.
[31] C. Denkert, J. Budczies, G. von Minckwitz, S. Wienert, S. Loibl, F. Klauschen, Strategies for developing Ki67 as a useful biomarker in breast cancer, Breast 24 (2015) S67–S72.
[32] J.H. Park, M.G. Rasch, J. Qiu, I.K. Lund, M. Egeblad, Presence of insulin-like growth factor binding proteins correlates with tumor-promoting effects of matrix metalloproteinase 9 in breast cancer, Neoplasia 17 (2015) 421–433.